Korean J. Chem. Eng., 38(9), 1903-1912 (2021)
DOI: 10.1007/s11814-021-0851-z

pISSN: 0256-1115
eISSN: 1975-7220

Corrosion inhibition of aluminum under basic conditions using *Medicago sativa L.* extract - thermodynamic studies

Rajamohan Natarajan† and Fatma Al Shibli

Chemical Engineering Section, Faculty of Engineering, Sohar University, Sohar, Oman
(*Received 28 February 2021 • Revised 2 May 2021 • Accepted 18 May 2021*)

Abstract−In this research, corrosion inhibitors were synthesized using locally available biomass, alfalfa plant. The inhibitor performance was evaluated at different operating conditions and the effect of process variables, namely inhibitor concentration (1-5%v/v), operating temperature (308.15-328.15 K) and method of extraction (alcohol and aqueous) were studied. The corrosion rate of aluminum decreased with increase in inhibitor concentration and the best result attained was 3.7 mg cm^{-2} h^{-1} with 5%v/v AALE and 308.15 K. The increase in temperature resulted in the decrease in inhibition efficiency, which could be related to detachment of inhibitors at elevated temperatures. The Langmuir adsorption Isotherm fitted well to the corrosion experiment data (R^2>0.990) and thermodynamic parameters were calculated. The value of separation factor ($0<R_L<1$) confirmed the favorable adsorption of corrosion inhibitor on the metal surface. Surface characterization of the green inhibitor using scanning electron microscopy was conducted to understand the morphology and FTIR spectrum was used to identify the main functional groups for Alfalfa extracts. The alcoholic extract possessed comparatively higher number of surface-active groups and produced better performance than aqueous extract. Arrhenius plots were employed to determine the activation energy. Tafel plot was used to determine theoretical corrosion current and potential. Electrochemical impedance spectroscopy inhibition efficiency was found to be 90.91% with 5% AALE.

Keywords: Corrosion, Inhibition, Metal, Green, Aluminum

INTRODUCTION

Industrial and domestic applications of metals as a construction material have increased significantly due to their unique beneficial properties related to high thermal conductivity, enhanced electrical properties and favorable mechanical properties. Aluminum, one of most widely used metals in manufacturing industries, is preferred for its corrosion resistance, alloy forming ability and cheaper cost. Moreover, it can be modified into various physical forms to suit the end-user requirements [1]. Corrosion of aluminum, which is a serious challenge faced in the industrial environment, results in material loss and replacement, which is reported to affect the metallurgical operations [2,3]. Corrosion is an undesirable electrochemical reaction that alters the surface properties of the metals and affects the physical and electrical properties [4]. Aluminum alloys are popular due to favorable mechanical properties and enhanced corrosion resistance. On the other hand, metallic aluminum has poor corrosion resistance under acidic, basic or marine conditions. Thus, the protection of aluminum from corrosion has become a key priority for industries. Corrosion inhibition, a method to prevent or reduce the extent of corrosion, is the technological solution for protecting the metals [5-7]. Corrosion inhibitors, classified as organic and inorganic inhibitors [8], have their unique chemical properties which aid in prevention of corrosion reactions. Organic inhibitors contain polar functional groups like -NO_2, -NH_2, -$CONH_2$ and -OH, promoting interactions between metal surface and inhibitors [9]. In spite of cost effectiveness, efficient inhibition under all operating conditions is not achieved [10]. Inorganic corrosion inhibitors are metallic salt-based compounds which are widely used for corrosion prevention. Use of organic and inorganic corrosion inhibitors is less preferred due to their toxic composition and effect on human health [11]. Effectiveness of inhibitors relies on the size of the organic particle, aromatic ring existence in the inhibitor molecule or the conjugated bound, carbon-chain length, type of bonding and functional groups consisting of heterocyclic and aliphatic components. Green corrosion inhibitors present an eco-friendly and cost-efficient alternative for corrosion inhibition methods. Green corrosion inhibitors are synthesized from naturally available biomass, mainly from plant sources [12-14]. The natural extracts of the plants are rich in compounds like terpenes, alkaloids, and polyphenols. Presence of functional groups involving atoms like N, O, S and P serves as active sites for the corrosion prevention on the metal surface [15-17]. Studies involving green corrosion inhibitors like Piper longum extract for aluminum in NaOH solution [19], chitosan for steel in chloride solution [20] and different bark extracts on aluminum in alkaline solution [21] have been reported. There is no reported literature on the application of alfalfa for corrosion inhibition of aluminum under basic conditions. In this research study, a novel green corrosion inhibitor was synthesized using alfalfa, a locally available agricultural crop. The cheap cost and local availability of alfalfa enhanced the economic feasibility of this method. The alfalfa leaves were utilized to

†To whom correspondence should be addressed.
E-mail: rnatarajan@su.edu.om

synthesize a corrosion inhibitor and tested for aluminum under basic conditions. The performance of the green inhibitor was evaluated using weight loss measurements. Equilibrium studies were conducted to determine the mechanism of surface coverage. The electrochemical mechanism of corrosion was studied using potentiodynamic and electrochemical impedance spectroscopy (EIS) methods. Thermodynamic studies were conducted to verify the feasibility of the process. The corrosion inhibitor was characterized to identify the surface-active functional groups through Fourier transform infra-red spectroscopy (FTIR) and metal surface was analyzed using scanning electron microscopic Imaging.

MATERIALS AND METHODOLOGIES

1. Preparation of Alfalfa Extracts Solution

Alfalfa (*Medicago sativa L.)* is an important agricultural crop, cultivated as fodder, in Oman. It is a perennial herb that lasts from 15 to 20 years or more in a dry climate and the length of the plant varies from 60-90 cm. The leaves of the plant are collected and washed to remove impurities like soil. The cleaned leaves are dried in sunlight for 24 h and powdered in a blender. The powdered leaves were sieved and the desired size fraction (>0.60 mm) was separated. The finely powdered sample was refluxed under boiling conditions with water for 1 h. The reflux mixture was filtered and the clear extract (named Alfalfa Aqueous Extract, AAE) was stored for further use as corrosion inhibitor. In the second method, the extraction was carried out with ethyl alcohol for a period of 1 h. The resultant extract (named Alfalfa Alcoholic Extract, AALE) was filtered and used.

2. Test Specimen and Gravimetric Measurements

The chemical composition of the aluminum sheet used in this experiment was as follows: Al (99.94%), Cu (0.02%), Mg (0.01%), Si (0.03%), Mn (0.003%) and Zn (0.004%) (wt%). The specimens used in the study were cut from an aluminum sheet into the required dimension, 1 cm×1 cm. With the aid of sandpaper (600, 800, 1,000 and 1,200 grit), the specimens were cleaned by buffing to create a smooth surface followed by cleaning with acetone. Subsequently, they were soaked in distilled water for about 30 seconds and then placed on a paper towel for 10 min to air dry. To remove any corrosion agents, specimens were rinsed with ethyl alcohol after each examination. The cleaned specimens were stored in moisture-free desiccators and weighted carefully before use. Weight loss experiments were performed at different inhibitor concentrations (1-5%), temperature (308.15-328.15 K), with a total immersion time of 1 h. Triplicate experiments were conducted under the same conditions in each case to ensure the consistency of the results and the average value was reported.

The rate of aluminum corrosion (CR) was estimated using Eq. (1):

$$CR = \frac{\Delta w}{S \cdot t} \quad (1)$$

where Δw is the weight loss (mg) of the aluminum samples, S is the total area of one aluminum specimen (cm^2) and t is the time of immersion (60 min).

The percentage inhibition efficiency (IE%) was calculated using Eq. (2):

$$IE\% = \frac{W_o - W}{W_o} \times 100 \quad (2)$$

where W_o and W are the corrosion rates ($mg \cdot cm^{-2} \cdot h^{-1}$) in the absence and presence of the inhibitor, respectively.

3. Electrochemical Measurements

The electrochemical experiments were conducted using a potentiostat/galvanostat (PARSTAT 2270). These tests were carried out in a standard three-electrode cell. The reference and counter electrodes used were saturated calomel electrode (SCE) and platinum (1 cm^2) . Functional electrodes are made of aluminum with uncovered areas of 1 cm^2. The electrode potential was stabilized for 30 minutes prior to the measurements. Both tests were carried out at room temperature. At open circuit potential, electrochemical impedance spectroscopy (EIS) measurements were performed in the frequency range of 1 kHz to 100 mHz with an amplitude of 10 mV. The diameter of the semicircles in the Nyquist plots was used to calculate charge transfer values. The electrochemical impedance spectroscopy inhibition efficiency (IE_{EIS}%) was calculated using Eq. (3):

$$IE_{EIS}\% = \frac{R_t - R_{to}}{R_t} \times 100 \quad (3)$$

where R_{to} and R_t are the charge transfer resistance (Ω) in the absence and presence of the inhibitor, respectively. At a scan rate of 1 mV/s, polarization curves were measured in the potential range of +250 to −250 mV with respect to the open circuit potential. Tafel extrapolation process was used to acquire electrochemical parameters such as E_{corr}, I_{corr}, and cathodic Tafel slopes (β_a and β_c). The potentiodynamic polarization inhibition efficiency (IE_P%) was calculated using Eq. (4):

$$IE_P\% = \frac{i_o - i}{i_o} \times 100 \quad (4)$$

where i_o and i are the corrosion current densities ($mAcm^{-2}$) in the absence and presence of the inhibitor, respectively.

4. Characterization Studies

The novel green corrosion inhibitor synthesized from alfalfa extract was characterized to identify the active functional groups by using FTIR. The sample analysis was performed using KBr pellets (PerkinElmer Spectrum BX, UK). The surface properties of the metal samples before and after addition of corrosion inhibitor were studied by SEM imaging (Jeol, Japan) with an accelerating voltage of 20 kV at high vacuum mode.

RESULTS AND DISCUSSION

1. FTIR Studies

The FTIR spectra of the AALE and AAE are presented in Figs. S1(a) and (b) (Supporting Data), respectively. The extracts contained organic compounds which played a vital role in adsorption onto the metal surface preventing corrosion. The main functional groups identified with AALE were O-H stretch (3,326 cm^{-1}, C-H stretch (2,974 cm^{-1}), alkyl ketone (1,274 cm^{-1}), C-O (1,327 and 1,380 cm^{-1}), alkyl amine (1,087 cm^{-1}) and C-C (879 cm^{-1}). The main functional groups identified with AAE were carboxylic acid (3,276 cm^{-1}) and

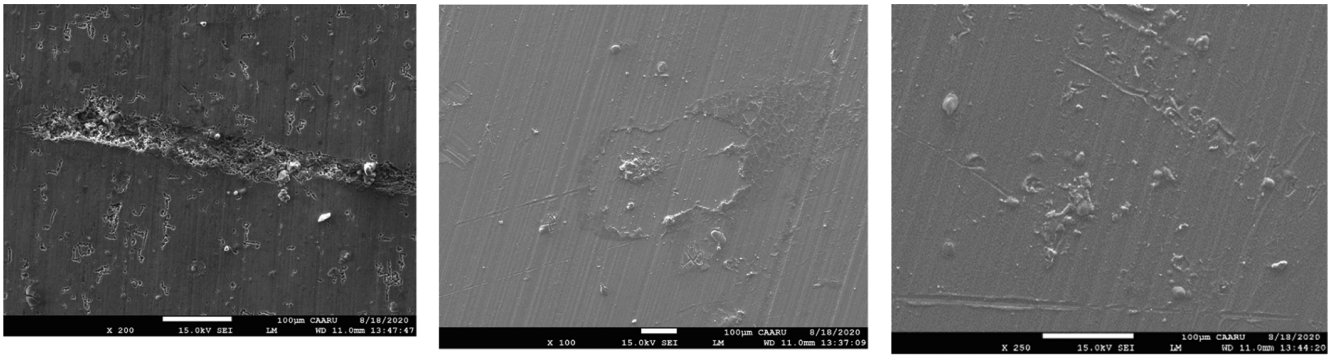

(a) (b) (c)

Fig. 1. (a) Aluminum specimen without corrosion inhibitor, (b) Aluminum specimen with AALE, (c) Aluminum specimen with AAE.

C=C stretch (1,635 cm^{-1}).

2. SEM Imaging

The metal samples with and without AALE addition were analyzed for the microstructure using SEM imaging. The aluminum specimen without the addition of corrosion inhibitor, shown in Fig. 1(a), displayed internal cracks and depletion of surface because of corrosion. As shown in Figs. 1(b) and 1(c), the samples exposed to corrosion inhibitor exhibited a smooth surface without any surface deformity and cracks. Through this study, it was observed that the corrosion inhibitor reduced the extent of corrosion significantly.

3. Effect of Inhibitor Concentration

In the first set of experiments, the effect of inhibitor concentration was studied in the range of 1-5% at fixed temperature. The performance of the green corrosion inhibitor was investigated in terms of weight loss measurements and the results are presented in Table 1. At an operating temperature of 308.15 K, the weight loss observed with the aluminum metal decreased with increasing inhibitor concentration [19], with both the inhibitors, namely AALE and AAE. The inhibition efficiency achieved with the addition of AALE increased from 72.4% to 92.4% in the extract concentration range of 1-5%v/v. The inhibition observed with AALE was found to be comparatively lesser with maximum efficiency of 73.4% achieved at 5%v/v. The weight loss measurements obtained were 19.33 and 36.33 mg cm^{-2} with AALE and AAE, respectively. These values were appreciably high compared with the loss of 70.0 mg·cm^{-2} obtained in the absence of inhibitors. The comparatively better performance of AALE is related to the presence of additional functional groups (between 879-1,380 cm^{1}), as shown in Fig. S1(a). The corrosion rate showed consistent decrease with increased addition of inhibitors [22]. The reduced corrosion rates of 3.9 and 7.3 mg

Table 1. Corrosion parameters for aluminum in 1 M NaOH in the absence and presence of different concentrations of Alfalfa extracts

Temp. (K)	Inhibitor conc. % (v/v)	Weight loss (mg·cm^{-2})		IE (%)		CR (mg·$cm^{-2}h^{-1}$)	
		AALE	AAE	AALE	AAE	AALE	AAE
308.15	1 M NaOH (Blank)	70.0		_		14.0	
	1	19.33	36.33	72.4	48.1	3.9	7.3
	2	12.33	28.33	82.4	59.5	2.5	5.7
	3	9.33	24.33	86.7	65.2	1.9	4.9
	4	8.33	22.33	88.1	68.1	1.7	4.5
	5	5.33	18.33	92.4	73.8	1.1	3.7
318.15	1 M NaOH (Blank)	90.0		_		18.0	
	1	31.33	48.33	65.2	46.3	6.3	9.7
	2	24.33	40.33	73.0	55.2	4.9	8.1
	3	21.33	36.33	76.3	59.6	4.3	7.3
	4	20.33	34.33	77.4	61.9	4.1	6.9
	5	15.33	28.33	83.0	68.5	3.1	5.7
328.15	1 M NaOH (Blank)	124.0		_		24.8	
	1	56.33	71.33	54.6	42.5	11.3	14.3
	2	48.33	62.33	61.0	49.7	9.7	12.5
	3	45.33	58.33	63.4	53.0	9.1	11.7
	4	44.33	56.33	64.2	54.6	8.9	11.3
	5	39.33	50.33	68.3	59.4	7.9	10.1

Table 2. Comparison with other research

Green corrosion inhibitor	Metal tested and conditions	Inhibition efficiency (IE%)	Reference
Piper longum extract	Aluminum in NaOH solution	94%	[12]
Stem bark extract	Aluminum Alloy in NaOH solution	85.3%	[13]
Stem Extract of *Bacopa Monnieri*	Aluminum in NaOH Solution	94%	[34]
Medicago sativa L. extract	Aluminum in NaOH solution	92%	This study
Sunflower seed hull extract	Mild steel in HCl solution	98%	[21]
Phoenix dactylifera extract	mild steel in 1M HCl solution	98%	[3]
Chitosan	Mild steel in sulfamic acid	90%	[23]
Musa Paradisica peel extract	Mild steel in HCl solution	90%	[27]

cm^{-2} h^{-1} observed with 1% v/v inhibitor concentration proved the effectiveness of the green corrosion inhibitor even at low concentrations. The studies conducted at elevated temperatures, 318.15 and 328.15 K, showed that the weight loss increased with increase in temperature and the corrosion rates increased. The increase in the efficacy of inhibition by *Medicago sativa L.* extracts was assessed by the weight loss methodology. Increasing extract concentration suggests that the extract is adsorbed on the aluminum surface at a higher concentration, resulting in greater surface coverage. Studies on the corrosion inhibition effect of different bark extracts on aluminum in alkaline solution reported an equivalent behavior [20]. The reduction of inhibition efficiency was noticed at all inhibitor concentrations and the values obtained at 5%v/v of AALE decreased to 68.3%, which is approximately 24% less than the results observed at 308.15 K. Similarly, the inhibition efficiency observed at 5%v/v of AALE decreased to 59.4%. The decline in inhibition efficiency along with the temperature rise despite the additive inhibitor dosage concentration is related to the electrostatic interaction. The green inhibitor extract minimized the corrosion rate for every tested inhibitor dosage through the role of functional groups attachment and created a barrier layer separating the metal surface from the corrosive solution [23,24]. Studies on corrosion inhibition reported similar effects of inhibitor concentration on corrosion rate and inhibition efficiency [25,26]. Alfalfa leaf juice protein concentrates were also found to have desirable foaming, emulsification, and gelling properties [27]. The results obtained in this study are compared with other related studies in Table 2. The inhibition efficiency results achieved in this study are comparable with other green corrosion inhibitors and confirm the suitability of industrial aluminum components.

4. Isotherm Studies

Equilibrium studies were performed to determine the surface coverage of the inhibitor and mechanism of sorption on the surface [20]. To understand the principles of interaction between the green inhibitor and the metal specimen in the inhibited corrosive medium, AALE and AAE inhibition processes were conducted at 308.15, 318.15 and 328.15 K, and the surface coverage fraction (θ) was calculated using Eq. (5) and recorded at different operating conditions.

$$\theta = \frac{IE\%}{100} \tag{5}$$

The Langmuir adsorption isotherm, representing the monolayer adsorption, is given by Eq (6).

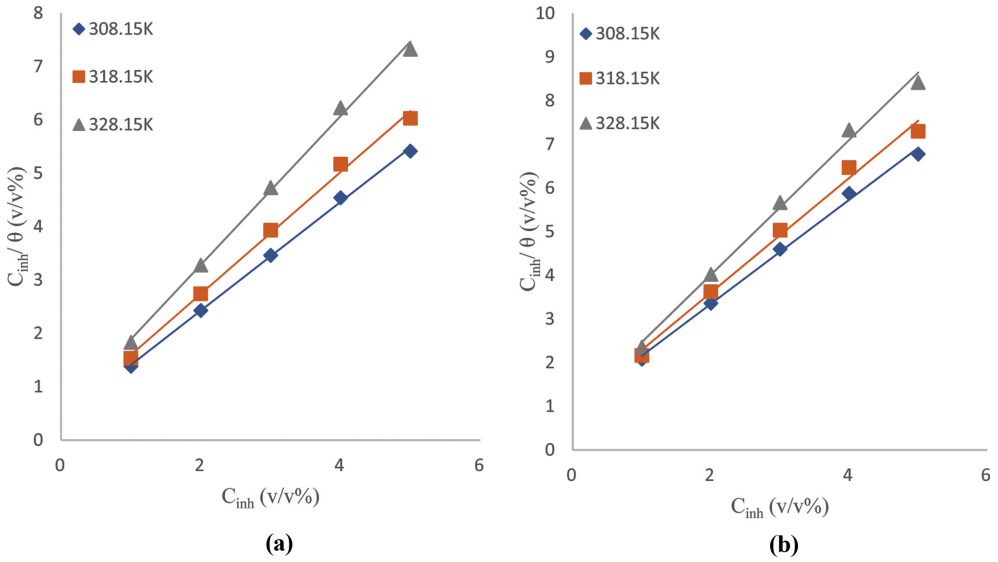

Fig. 2. Langmuir adsorption isotherm plot for corrosion of aluminum in 1 M NaOH containing different concentration of (a)AALE and (b) AAE.

Table 3. The values of dimensionless separation factor R_L for alfalfa extracts

Temperature (K)	Concentration %(v/v)	AALE		AAE	
		K_L	R_L	K_L	R_L
308.15	1	2.5484	0.2818	1.1851	0.4576
	2		0.1640		0.2967
	3		0.1157		0.2195
	4		0.0893		0.1742
	5		0.0728		0.1444
318.15	1	2.1891	0.3136	1.0997	0.4762
	2		0.1859		0.3125
	3		0.1321		0.2326
	4		0.1025		0.1852
	5		0.0837		0.1539
328.15	1	2.0048	0.3328	1.1119	0.4735
	2		0.1996		0.3102
	3		0.1426		0.2307
	4		0.1109		0.1836
	5		0.0907		0.1525

Table 4. Thermodynamic parameters for the dissolution of aluminum in 1 M NaOH

T (K)	AALE				AAE			
	R^2	ΔG^o_{ads} (KJ mol^{-1})	ΔH^o_{ads} (KJ mol^{-1})	ΔS^o_{ads} (KJ $mol^{-1}K^{-1}$)	R^2	ΔG^o_{ads} (KJ mol^{-1})	ΔH^o_{ads} (KJ mol^{-1})	ΔS^o_{ads} (KJ $mol^{-1}K^{-1}$)
308.15	0.999	−12.60	−8.441	41.142	0.997	−10.72	−26.099	34.720
318.15	0.996	−12.70		39.906	0.992	−10.88		34.183
328.15	0.997	−12.86		39.175	0.995	−11.25		34.274

$$\frac{C_{inh}}{\theta} = \frac{1}{K_L} + C_{inh} \quad (6)$$

where C_{inh} denotes the inhibitor concentration (%v/v) and K_L is the Langmuir equilibrium constant of adsorption. The Langmuir adsorption isotherm plot for corrosion of aluminum in 1 M NaOH containing different concentrations of AALE and AAE (C_{inh}/θ versus C_{inh}) is represented in Figs. 2(a) and (b). The experimental data fitted very well with isotherm plot (R^2>0.990), and the minor deviations from unity can be related as the interaction between the adsorbed species on the metal surface [28]. The Langmuir isotherm confirmed the monolayer coverage of the green inhibitor. A single water molecule adsorbed is substituted on the aluminum surface by one molecule of the adsorbate inhibitor [29,30]. The K_L values decreased with increase in temperature with both the extracts, indicating physical adsorption upon the aluminum surface. A comparable result is reported in the studies which employed chitosan as a green corrosion inhibitor [31]. In addition, the Langmuir isotherm suitability can be expressed in terms of a dimensionless separation factor, R_L, and defined by Eq. (7):

$$R_L = \frac{1}{1 + K_L C_{inh}} \quad (7)$$

From Table 3, it was observed that all R_L values are lower than unity (≤0.332 for AALE and ≤0.476 for AAE) and confirmed the desirable adsorption processes. Similar behavior was observed in the studies using apricot juice as a green corrosion inhibitor of mild steel in phosphoric acid [32].

5. Thermodynamic Studies

The feasibility of the corrosion process, in relation to extent of adsorption, was verified by thermodynamic experiments [33]. The standard free energy of adsorption (ΔG^o_{ads}) is calculated using Eq. (8):

$$\Delta G^o_{ads} = -2.303RT \log 55.5K_L \quad (8)$$

The estimated free energy of adsorption (ΔG^o_{ads}) is given in Table 4 and the negative ΔG^o_{ads} results in both extracts confirmed spontaneous coverage of aluminum surface by the green inhibitor and interaction between extract components and aluminum surface [34,35]. The observed value of ΔG^o_{ads} equal or less than −20 KJ/mol is usually associated with physical adsorption [35]. Thus, the mechanism of adsorption associated with this study is physical adsorption. The free energy of adsorption is interrelated with entropy and enthalpy of adsorption process, and given below in Eq. (9):

$$\Delta G^o_{ads} = \Delta H^o_{ads} - \Delta S^o_{ads} T \quad (9)$$

where ΔH^o_{ads} is the enthalpy of adsorption (KJ mol^{-1}) and ΔS^o_{ads} is the entropy of adsorption (KJ $mol^{-1}K^{-1}$). As found in Table 3, the values of ΔH^o_{ads} are negative and the adsorption of inhibitor onto the aluminum surface was found to be exothermic. The absolute

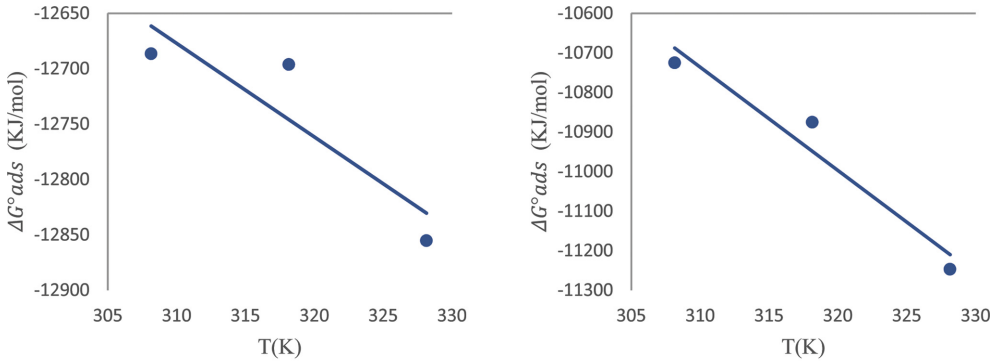

Fig. 3. ΔG^{o}_{ads} against temperature plot for adsorption of (a) AALE and (b) AAE on metal surface.

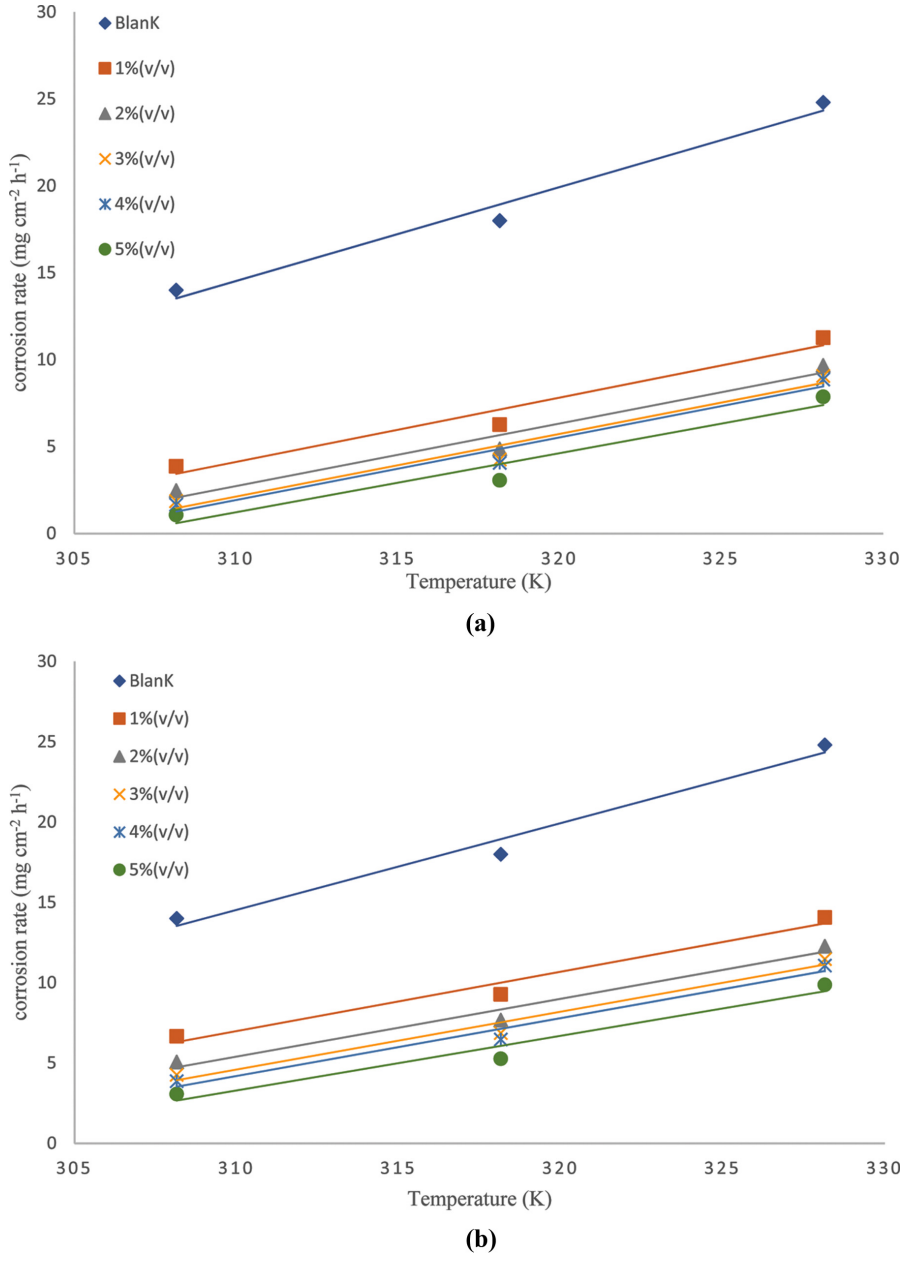

Fig. 4. Effect of temperature on dissolution of aluminum in 1 M NaOH (a) AALE and, (b) AAE.

value of ΔH^{o}_{ads} for the physical adsorption should be lower than 40 KJ mol^{-1} [36] and the results obtained in this study confirm the suitability of physical nature of sorption process. Entropy of adsorption (ΔS^{o}_{ads}) was found to be positive values and increased with increase in temperature. This observation indicates that the disorder is increasing with increase in temperature.

6. Effect of Temperature and Activation Energy Determination

The effect of temperature on the rate of dissolution of aluminum in 1 M NaOH containing different concentration of AAE and ABWE was tested by weight loss method over a temperature range of 308.15-328.15 K. The data indicated that, both in the absence and presence of extract, there is a rise in corrosion rate along with elevation in temperature [37]. In the absence of extract, the corrosion rate is higher at all examined temperatures, suggesting more interaction of the free alkaline solution with the metal surface [38, 39]. The enhancement of corrosion rate at higher temperatures could be related to de-activation of inhibitor functional groups [40]. The corrosion rate variations were recorded for inhibition studies using AALE and AAE and shown in Figs. 4(a) and (b), respectively. The AAE showed lower tendency to reduce corrosion rate compared to AALE at the same condition.

The activation energy of the corrosion process is calculated using the Arrhenius equation and given by Eq. (10):

$$\log C_R = \log A - \left(\frac{E_a}{2.303RT}\right) \quad (10)$$

The activation energy (E_a) of the corrosion experiments in the absence and presence of alfalfa extracts is determined from the plot of log C_R versus 1/T. The slopes of the straight-line plots (Figs. 5(a) and (b)) are used to determine the activation energy. The val-

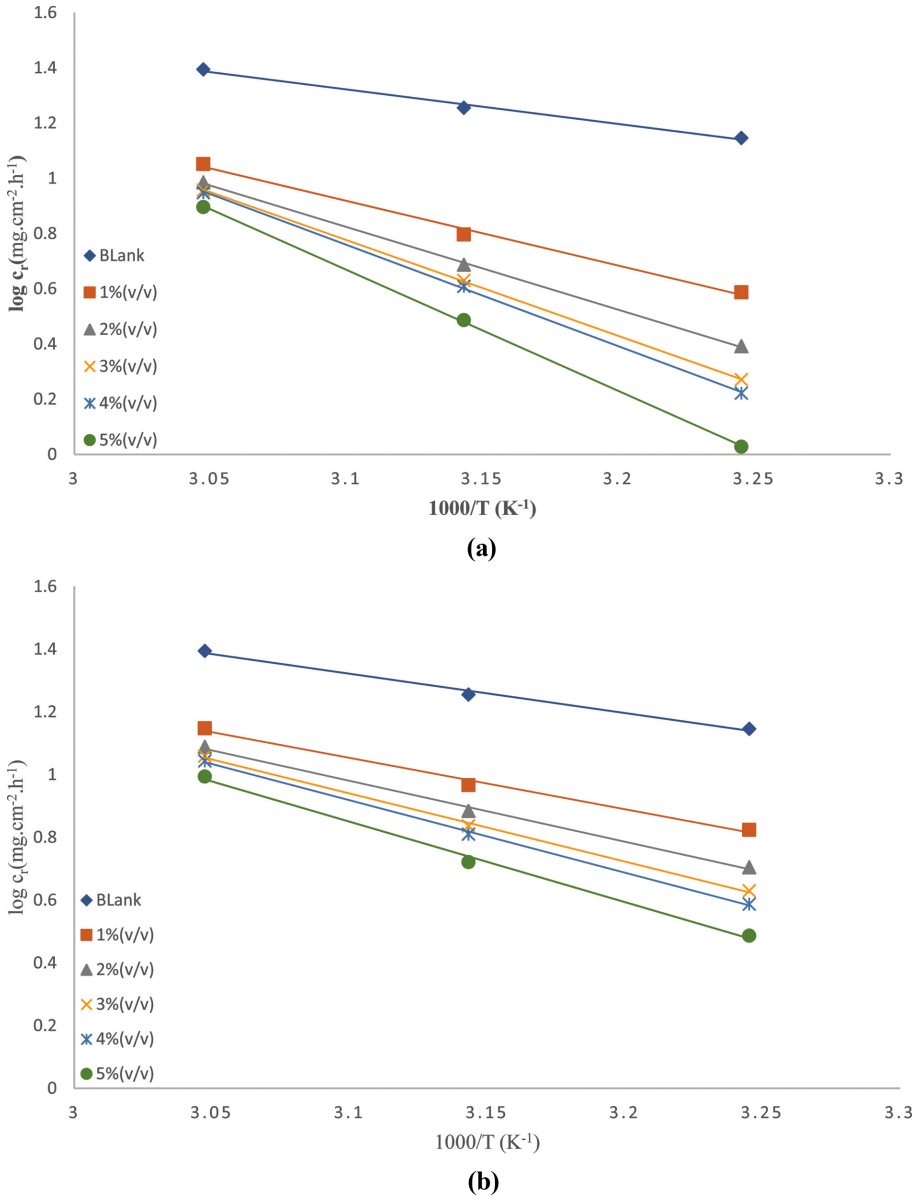

Fig. 5. Arrhenius plots of the corrosion rate for aluminum in alkali medium in absence and presence of different concentration of (a) AALE and (b)AAE.

Table 5. Activation energy for the dissolution of aluminum in 1 M NaOH in the absence and presence of different concentrations of Alfalfa Extracts

Concentration %(v/v)	AALE	AAE
	Ea×10^{-4} (KJ mol^{-1})	Ea×10^{-4} (KJ mol^{-1})
Blank	2.400	2.400
1	4.490	3.134
2	5.740	3.714
3	6.646	4.153
4	7.030	4.419

ues of E_a>20 KJ/mol, observed in this study (shown in Table 5) suggest that the inhibition process is a surface interaction-based process [41]. The changes in activation energy in the presence of AALE and AAE confirm organic green corrosion inhibitor adsorption on the examined metal surface and increased energy barrier for the corrosion process The activation energy increased from 2.400 KJ mol^{-1} (blank) to 8.403 KJ mol^{-1} (5%v/v AALE) and 4.908 KJ mol^{-1} (5%v/v AAE), respectively. Studies on aluminum corrosion inhibition using *Bacopa monnieri* stem extract reported an increase in activation energy from 15.9 KJ·mg^{-1} (llank) to 81.8 KJ·mg^{-1} (in presence of 400 mg·L^{-1} inhibitor) [42].

7. Inhibition Mechanism

The extract of *Medicago sativa L.* contains a variety of naturally occurring compounds. Aluminum sheets have an amorphous alumina oxide layer that thickens when exposed to an aqueous solution, eventually becoming crystalline hydrated alumina. The method of aluminum dissolution in alkali solution is as follows (Eq. (11)):

$$2Al_{(s)}+\frac{3}{2}O_{2(g)}\leftrightarrow Al_2O_{3(s)} \quad (11)$$

The resulting oxide film serves as a static shield, separating the metal from the solution. Alkaline solutions, on the other hand, are believed to degrade its properties. The breakdown of aluminum in an alkali solution is explained by the reaction (Eq. (12)) given below:

$$Al+3H_2O+OH^-\rightarrow\frac{3}{2}H_2+[Al(OH)_4]^- \quad (12)$$

The metal dissolves due to the formation of a soluble complex ion. Adsorption of inhibitors at the surface of the aluminum, which arises by eliminating water molecules, is facilitated mostly by the inclusion of heteroatoms, -OH pairs, and pi ties [43,44]. The better inhibitory performance of the *Medicago sativa L.* extract is due to the functional groups, which occupy a large region on the Aluminum surface.

8. Electrochemical Measurement

8-1. Potentiodynamic Polarization Studies

Polarization curves for aluminum in alkali medium in the absence and presence of different concentrations of (a) AALE and (b) AAE were studied. The anodic and cathodic Tafel constants (β_a and β_c), corrosion potential (E_{corr}), and corrosion current density (i_{corr}) associated with polarization measurements were measured and mentioned in Table 6. In the presence, of AALE and

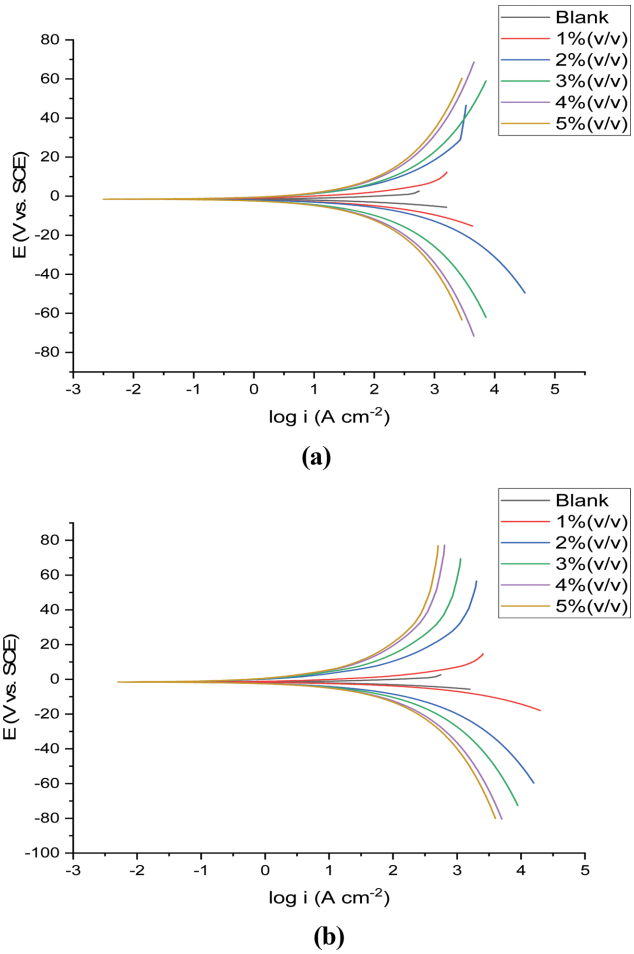

Fig. 6. Polarization curves for aluminum in alkali medium in absence and presence of different concentration of (a) AALE and (b)AAE.

AAE inhibitor extracts, both the anodic and cathodic curves shift forward towards lower current density, as shown in Figs. 6(a) and (b), respectively. With addition of inhibitors, i_{corr} values decreased and confirmed that the inhibitor molecules were adsorbed on the aluminum surface. As shown in Table 6, the i_{corr} decreased from 278 $mAcm^{-2}$ (blank) to 81.36 $mAcm^{-2}$ and 37.8 $mAcm^{-2}$ for AALE and AAE (5% v/v), respectively. The maximal deviation with addition AALE and AAE in this study was about 70-10 mV, which is less than 85 mV, implying that the inhibitors tested are of mixed type. Table 6 shows that the values of β_a and β_c decrease with increasing inhibitor concentration, with both the inhibitors, namely AALE and AAE. The β_a, achieved with the addition of AALE, decreased from 1.211 to 0.653 (V dec^{-1}) in the extract concentration range of 1-5%v/v. The β_a observed with AAE was found to be comparatively lesser with minimum β_a value of 0.891 V dec^{-1} achieved at 5%v/v. It was discovered that the drop in β_c could be due to the adsorption of an inhibitor molecule on the metal surface, which reduced the alkali attack. The reduction in β_a in the anodic case can be attributed to the change in the anodic dissolution mechanism related to the inhibitor module's adsorption on the active sites [45]. The anodic and cathodic slopes changed to

Table 6. Potentiodynamic polarization parameters and Impedance parameters for Aluminium in 1 M NaOH in the absence and presence of different concentrations of Alfalfa extracts

Concentration %(v/v)	Potentiodynamic polarization parameters										Impedance parameters			
	E_{corr} (V/SCE)		β_a (V dec^{-1})		β_c (V dec^{-1})		I_{corr} ($mAcm^{-2}$)		IE_P%		R_t Ω		IE_{EIS}%	
	AALE	AAE	AALE	AAE	AALE	AAE	AALE	AAE	AALE	AAE	AALE	AAE	AALE	AAE
Blank	1.55		1.1861		0.62		278		_		5		_	
1	1.53	1.62	1.211	1.052	0.790	0.570	96.18	148.22	65.40	46.68	19.0	9.4	73.68	46.81
2	1.53	1.59	1.031	1.119	0.760	0.680	87.84	121.38	68.40	56.33	27.0	12.0	81.48	58.33
3	1.54	1.58	0.977	1.004	0.740	0.630	59.21	107.54	78.70	61.31	28.0	13.8	82.14	63.77
4	1.54	1.58	0.839	0.994	0.730	0.600	52.54	98.67	81.10	64.50	30.0	15	83.33	66.67
5	1.51	1.56	0.653	0.891	0.650	0.590	37.8	81.36	86.40	70.73	55.0	18	90.91	72.22

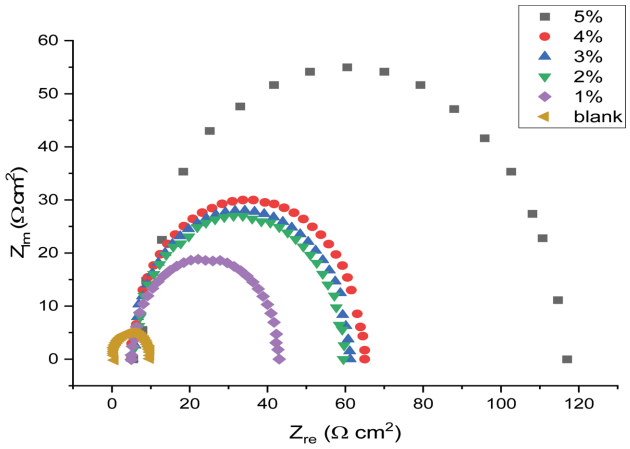

(a)

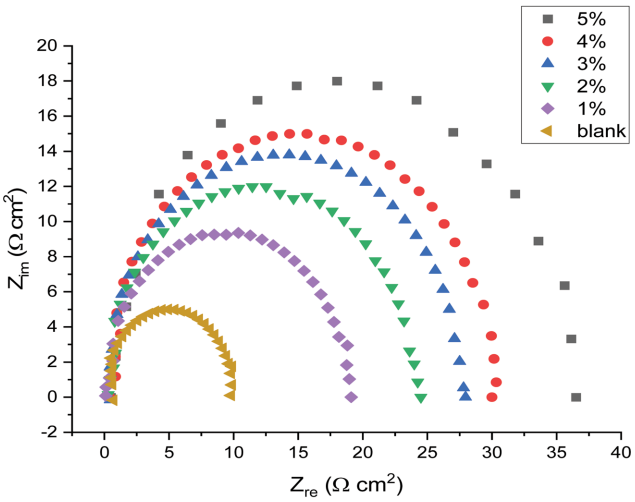

(b)

Fig. 7. Nyquist plots for aluminum in alkali medium in absence and presence of different concentration of (a) AALE and (b) AAE.

relatively low current density relative to the blank, and hence the inhibition efficiency (IE_P%) improved with increasing extract concentration, reaching maximum values of 86.40% for AALE and 70.73% for AAE at 5% (v/v).

8-2. EIS Measurements

The role of inhibitor concentration for aluminum corrosion in alkali medium was studied through EIS measurements and is represented in Fig. 7. With the addition of inhibitors, Nyquist plots revealed that the semicircle diameter increased. The value of R_t increased from 19 to 55 Ω for AALE, while the value of R_t increased 9.4 to 18 Ω for AAE, as seen in Table 6. This growth in capacitive semicircles indicates that the inhibitors' activity is due to their adsorption on the metal surface. At higher and lower frequency regions, the figure shows depressed capacitive semicircles, which are typical of the Randles circuit. The presence of an adsorbed intermediate on the surface is reported to result in inductive loops. As a result, adsorbed intermediate species like $Al^{+3}_{(ads)}$ and $Al^{+}_{(ads)}$ may be involved in the Al dissolution process. The redox Al-Al+ reaction was thought to be the rate-determining phase in the charge transfer mechanism, which explains the capacitive semicircle at higher frequencies [46]. Fig. 8 illustrates the corresponding Randles circuit model.

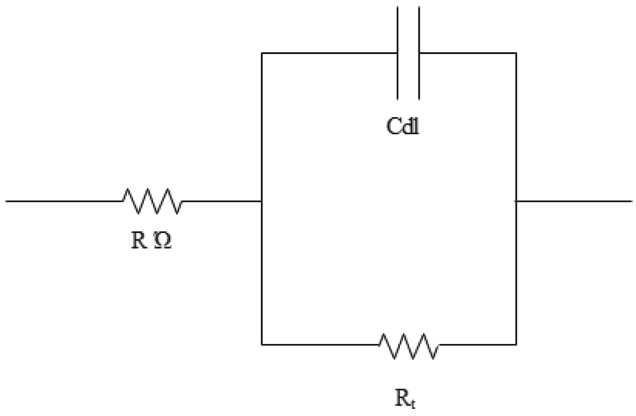

Fig. 8. Prescribed equivalent circuit schematic by Randles.

CONCLUSION

A novel green corrosion inhibitor was synthesized using *Medicago sativa L.* and utilized to prevent corrosion of aluminum in alkaline medium. The corrosion rate decreased and the inhibition efficiency increased with increase in inhibitor concentrations with both AALE and AAE. The maximum inhibition efficiency achieved was 92.4% at 5% v/v AALE concentration and 308.15 K. The mechanism of inhibitor sorption was found to be monolayer process as

confirmed by Langmuir isotherm. The negative values of Free energy of adsorption confirmed the alfalfa attachment to aluminum surface as a spontaneous adsorption process. Physical adsorption mechanism is suggested for AALE and AAE as the obtained values of ΔG^{o}_{ads} are lower than −20 KJ/mol. The temperature increase influenced the inhibitor efficiency negatively. Activation energy measurements were used to understand the reaction mechanism. The theoretical corrosion current was estimated and found to decrease with increase in green corrosion inhibitor concentration. Aluminum interaction with inhibitor was analyzed using impedance measurements. Thus, the alfalfa extract proved to be an efficient green corrosion inhibitor to control aluminum corrosion in alkaline environment.

ACKNOWLEDGEMENTS

The authors acknowledge the financial support provided to conduct the research studies by The Research Council of Oman and infrastructure provided by Sohar University.

SUPPORTING INFORMATION

Additional information as noted in the text. This information is available via the Internet at http://www.springer.com/chemistry/journal/11814.

REFERENCES

1. G. Asan and A. Asan, *J. Mol. Struct.*, **1201**, 127184 (2020).
2. I. O. Zvirko, S. F. Savula, V. M. Tsependa, G. Gabetta and H. M. Nykyforchyn, *Procedia Struct. Integrity*, **2**, 509 (2016).
3. E. A. Şahin, R. Solmaz, İ. H. Gecibesler and G. Kardaş, *Mater. Res. Express.*, **7(1)**, 016585 (2020).
4. C. Verma, J. Haque, M. A. Quraishi and E. E. Ebenso, *J. Mol. Liq.*, **275**, 18 (2019).
5. S. Bashir, A. Thakur, H. Lgaz, I. M. Chung and A. Kumar, *Arab. J. Sci. Eng.*, **45**, 4773 (2020).
6. S. Bashir, V. Sharma, H. Lgaz, I. M. Chung, A. Singh and A. Kumar, *J. Mol. Liq.*, **263**, 454 (2018).
7. P. Shetty, *Chem. Eng. Commun.*, **207**, 985 (2020).
8. S. Marzorati, L. Verotta and S. P. Trasatti, *Molecules*, **24**, 48 (2019).
9. M. Goyal, S. Kumar, I. Bahadur, C. Verma and E. E. Ebenso, *J. Mol. Liq.*, **256**, 565 (2018).
10. P. Jain, B. Patidar and J. Bhawsar, *J. Bio-and Tribo-Corrosion*, **6**, 1 (2020).
11. V. S. Saji and S. A. Umoren, *Corrosion inhibitors in the oil and gas industry*, Wiley-VCH (2020).
12. B. El Ibrahimi, A. Jmiai, L. Bazzi and S. El Issami, *Arabian J. Chem.*, **13**(1), 740 (2020).
13. S. Bashir, A. Thakur, H. Lgaz, I. M. Chung and A. Kumar, *J. Mol. Liq.*, **293**, 111539 (2019).
14. B. Tan, J. He, S. Zhang, C. Xu, S. Chen, H. Liu and W. Li, *J. Colloid Interface Sci.*, **585**, 287 (2021).
15. X. Zhang, W. Li, X. Zuo, B. Tan, C. Xu and S. Zhang, *J. Mol. Liq.*, **325**, 115214 (2021).
16. S. Bashir, A. Thakur, H. Lgaz, I. M. Chung and A. Kumar, *Surf. Interfaces*, **20**, 100542 (2020).
17. B. Tan, B. Xiang, S. Zhang, Y. Qiang, L. Xu, S. Chen and J. He, *J. Colloid Interface Sci.*, **582**, 918 (2021).
18. X. Zheng, M. Gong, Q. Li and L. Guo, *Sci. Rep.*, **8**, 1 (2018).
19. A. Singh, I. Ahamad and M. A. Quraishi, *Arabian J. Chem.*, **9**, S1584 (2016).
20. N. Chaubey, Savita, V. K. Singh and M. A. Quraishi, *J. Assoc. Arab Univ. Basic Appl. Sci.*, **22**(1), 38 (2017).
21. G. Cui, J. Guo, Y. Zhang, Q. Zhao, S. Fu, T. Han, S. Zhang and Y. Wu, *Carbohydr. Polym.*, **203**, 386 (2019).
22. M. R. Singh, P. Gupta and K. Gupta, *Arabian J. Chem.*, **12**, 1035 (2019).
23. C. Pan, M. Guo, W. Han, Z. Wang and C. Wang, *Corros. Eng. Sci. Techn.*, **54**(3), 241 (2019).
24. Y. Yaocheng, Y. Caihong, A. Singh and Y. Lin, *New J. Chem.*, **43**(40), 16058 (2019).
25. S. Kagatikar, B. P. Charitha and R. Padmalatha, *Surf. Eng. Appl. Electrochem.*, **56**(3), 381 (2020).
26. I. B. Onyeachu, I. B. Obot, A. A. Sorour and M. I. Abdul-Rashid, *Corros. Sci.*, **150**, 183 (2019).
27. M. P. Hojilla-Evangelista, G. W. Selling, R. Hatfield and M. Digman, *J. Sci. Food Agric.*, **97**, 882 (2017).
28. H. Lgaz, S. Masroor, M. Chafiq, M. Damej, A. Brahmia, R. Salghi and I. M. Chung, *Metals.*, **10**, 357 (2020).
29. H. Hassannejad and A. Nouri, *J. Mol. Liq.*, **254**, 377 (2018).
30. E. Naseri, M. Hajisafari, A. Kosari, M. Talari, S. Hosseinpour and A. Davoodi, *J. Mol. Liq.*, **269**, 193 (2018).
31. N. K. Gupta, P. G. Joshi, V. Srivastava and M. A. Quraishi, *Int. J. Biol. Macromo.*, **106**, 704 (2018).
32. A. S. Yaro, A. A. Khadom and R. K. Wael, *Alexandria Eng. J.*, **52**, 129 (2013).
33. O. A. Akinbulumo, O. J. Odejobi and E. L. Odekanle, *Results Mater.*, **5**, 100074 (2020).
34. K. S. M. Ferıgıta and F. Kandemirli, *Int. J. Glob. Sci. Res.*, **1**, 289 (2020).
35. G. Ji, S. Anjum, S. Sundaram and R. Prakash, *Corros. Sci.*, **90**, 107 (2015).
36. P. E. Alvarez, N. V. Fiori-Bimbi, A. Neske, S. A. Brandán and C. A. Gervasi, *J. Ind. Eng. Chem.*, **58**, 92 (2018).
37. S. Devikala, P. Kamaraj, M. Arthanareeswari and M. B. Patel, *Mater. Today. Proc.*, **14**, 580 (2019).
38. L. T. Popoola, *Corros. Rev.*, **37**, 71 (2019).
39. K. Xhanari and M. Finšgar, *Arabian J. Chem.*, **12**, 4646 (2019).
40. I. B. Obot, S. A. Umoren and N. K. Ankah, *J. Mol. Liq.*, **277**, 749 (2019).
41. Y. Sushmitha and P. Rao, *Port. Electrochim. Acta.*, **38**(3), 149 (2020).
42. A. Singh, E. E. Ebenso and M. A. Quraishi, *Int. J. Electrochem. Sci.*, **7**, 3409 (2012).
43. M. Akin, S. Nalbantoglu, O. Cuhadar, D. Uzun and N. Saki, *Res. Chem. Intermed.*, **41**, 899 (2015).
44. M. Abdallah, H. M. Altass, A. S. Al-Gorair, J. H. Al-Fahemi, B. A. A. L. Jahdaly and K. A. Soliman, *J. Mol. Liq.*, **323**, 115036 (2021).
45. X. Li, S. Deng and X. Xie, *Corros. Sci.*, **81**, 162 (2014).
46. D. Prabhu and P. Rao, *J. Environ. Chem. Eng.*, **1**, 676 (2013).

Supporting Information

Corrosion inhibition of aluminum under basic conditions using *Medicago sativa L.* extract - thermodynamic studies

Rajamohan Natarajan[†] and Fatma Al Shibli

Chemical Engineering Section, Faculty of Engineering, Sohar University, Sohar, Oman
(*Received 28 February 2021 • Revised 2 May 2021 • Accepted 18 May 2021*)

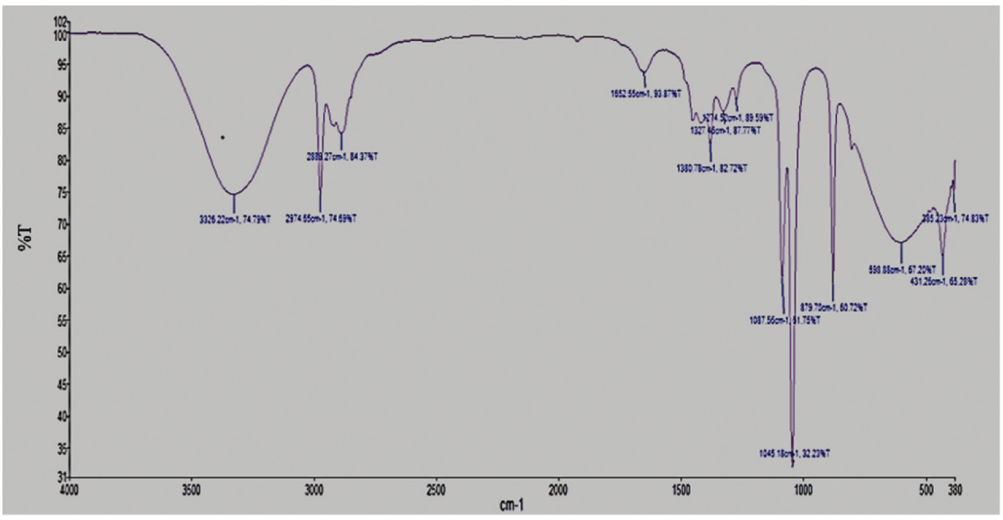

(a)

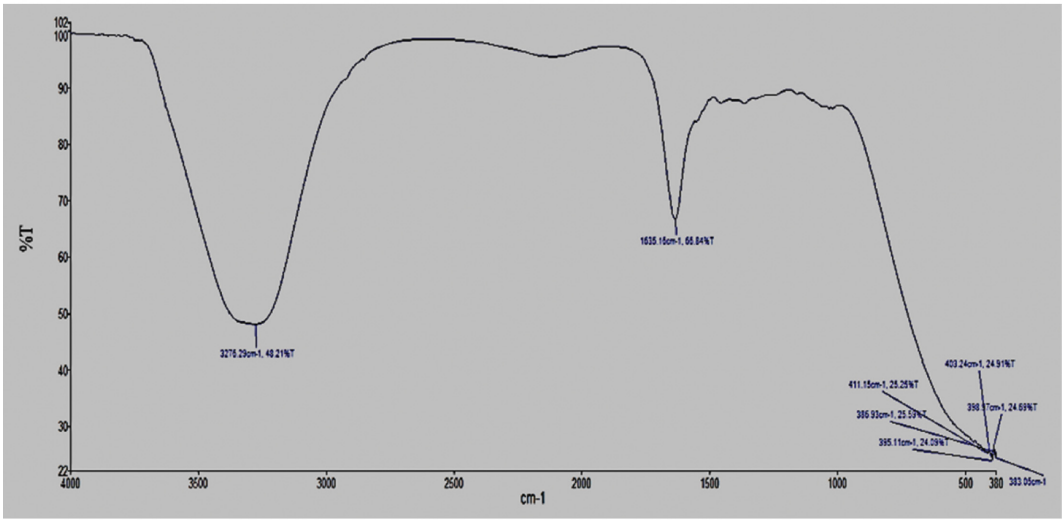

(b)

Fig. S1. (a) FTIR of AALE, (b) FTIR of AAE.